Electronic Supplementary Material (ESI) for Environmental Science: Nano.

Electron Supporting Information (ESI)

For

Molecular-Scale Determination of the Facet- and Adsorbent-Dependent Phosphate Adsorption by Metal-Based Adsorbents

Xinfei Ge, Lijun Wang, and Wenjun Zhang*

College of Resources and Environment, Huazhong Agricultural University, Wuhan 430070, China

***To whom correspondence should be addressed.**

Email: wenjunzhang@hzau.edu.cn

Number of Tables: 2

Number of Figures: 16

Number of Pages: 10

Table S1. Raman peak assignments of hematite and peptide.

Compound	Raman shift (cm^{-1})	Assignment
Hematite	225	A_{1g} (Fe-O sys. str.)
	245	E_g (Fe-O sys. bend)
	296	E_g (Fe-O sys. bend)
	412	E_g (Fe-O sys. bend)
	500	A_{1g} (Fe-O sys. str.)
	611	E_g (Fe-O sys. bend)
	1320	$2E_u$ (two-magnon scattering)
Peptide	1230-1340	Amide III
	1510-1570	Amide II
	1600-1700	Amide I

Table S2. Values of f_{eq} and ΔG_b obtained from fitting the Friddle-Noy-De Yoreo model to DFS data, which are shown as mean ± standard deviation (n = 3).

pH	KCl (mM)	Interaction	f_{eq} (pN)	ΔG_b (kJ/mol)
5	10	Ce-bound peptide	287.56±15.48	13.24±1.14
5	10	$(10\bar{1}0)$	243.21±11.32	10.7±0.84
5	10	$(11\bar{2}0)$	200.44±12.35	8.52±0.61
5	10	(0001)	150.78±9.87	6.61±0.42
5	10	Ce-bound peptide	287.56±15.48	13.24±1.14
7	10	Ce-bound peptide	231.67±10.21	10.2±0.84
9	10	Ce-bound peptide	188.58±8.64	7.78±0.73
5	10	$(10\bar{1}0)$	243.21±11.32	10.7±0.84
7	10	$(10\bar{1}0)$	201.36±11.21	8.86±0.58
9	10	$(10\bar{1}0)$	153.86±8.54	6.79±0.62
5	1	Ce-bound peptide	320.35±16.83	16.48±1.25
5	10	Ce-bound peptide	287.56±15.48	13.24±1.14
5	100	Ce-bound peptide	235.42±12.31	10.46±0.95
5	1	$(10\bar{1}0)$	295.48±13.56	13.21±1.01
5	10	$(10\bar{1}0)$	243.21±11.32	10.7±0.84
5	100	$(10\bar{1}0)$	188.76±6.98	8.42±0.36

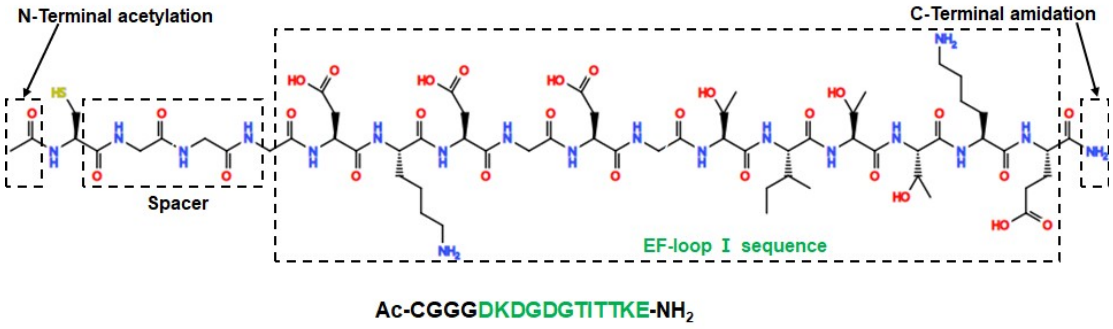

Figure S1. Chemical structure of peptide designed to bind Ce^{3+} ions, which consists of

N-terminal acetylation, spacer, EF-loop I sequence and C-terminal amidation.

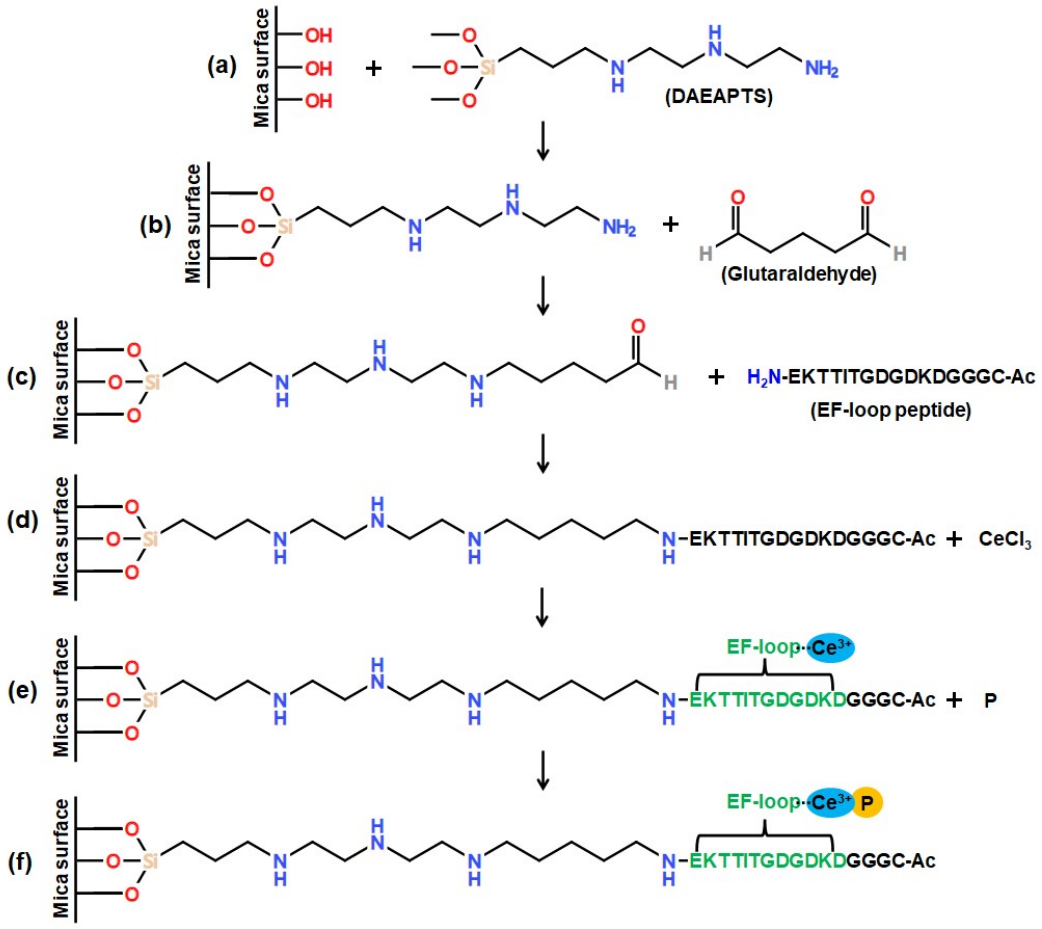

Figure S2. Schematic representation of (a-d) the peptide decoration on mica surface using trimethoxysilylpropyl-diethylenetriamine (DAEAPTS) and glutaraldehyde linker, (e) the specific binding of Ce^{3+} to peptide and (f) the adsorption of P by Ce-bound peptide. The decoration method involves: (a) mica substrates cleaning; (b) generation of silane layer using DAEAPTS solution; (c) treatment with glutaraldehyde solution; (d) addition of targeted peptide.

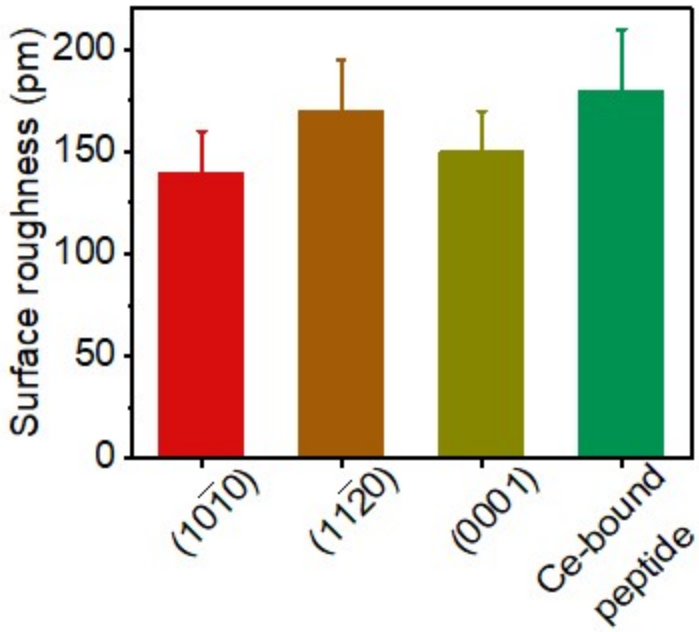

Figure S3. Significance analysis of roughness of the (10$\bar{1}$0), (11$\bar{2}$0) and (0001) surfaces of hematite and Ce-bound peptide surface decorated on mica.

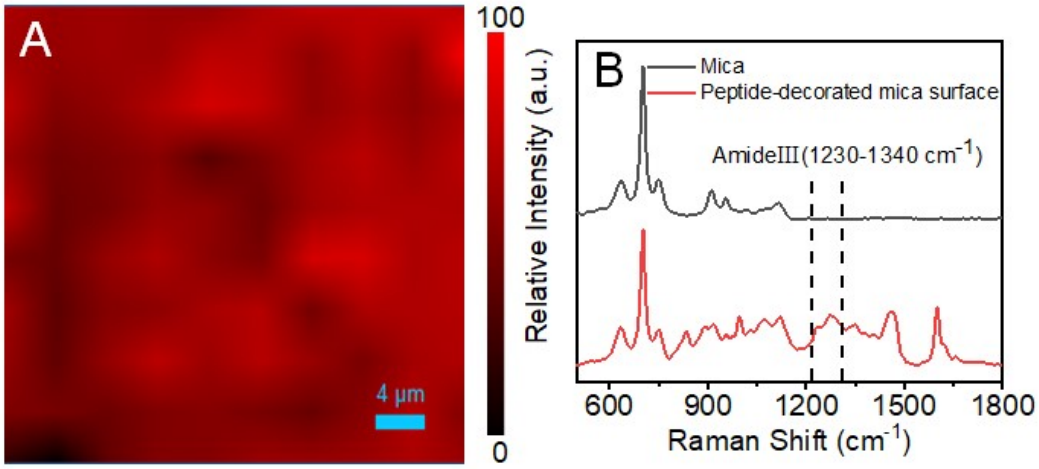

Figure S4. Peptide-decorated mica surface identified by (A) Raman mapping with (B) Raman characteristic vibration of Amide III (1230–1340 cm^{-1}).

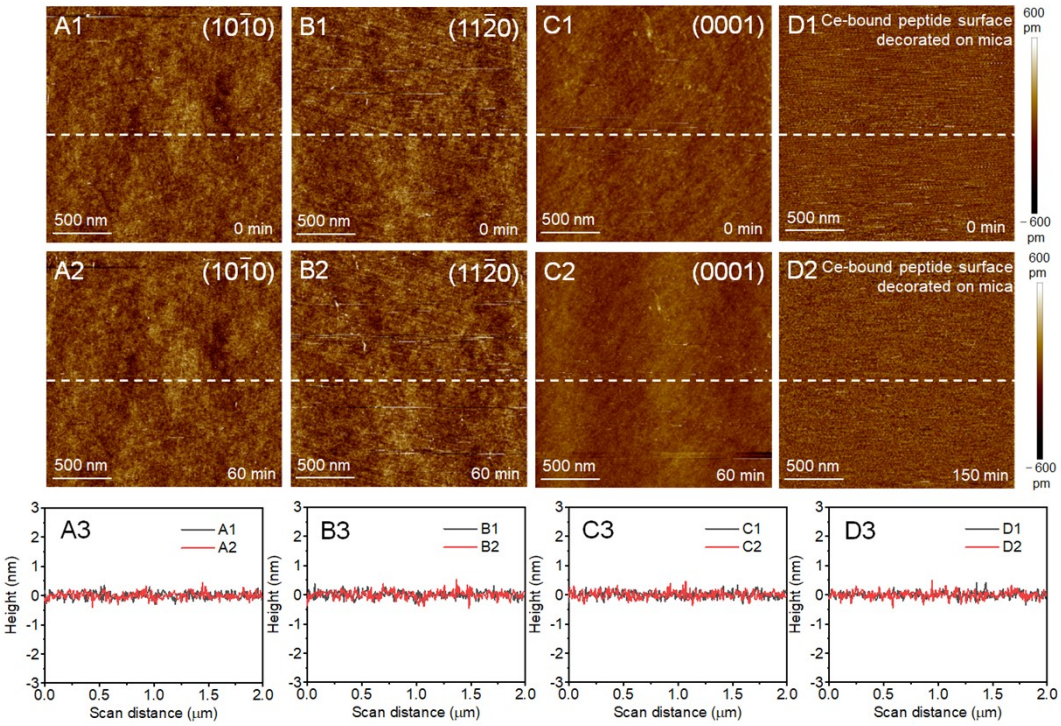

Figure S5. AFM height imaging and the corresponding height analyses of the (A1-A3) (10$\bar{1}$0), (B1-B3) (11$\bar{2}$0) and (C1-C3) (0001) surfaces of hematite and Ce-bound peptide surface decorated on mica before and after exposure to a simple P solution (100 mg/L KH_2PO_4; pH 5; 10 mM KCl).

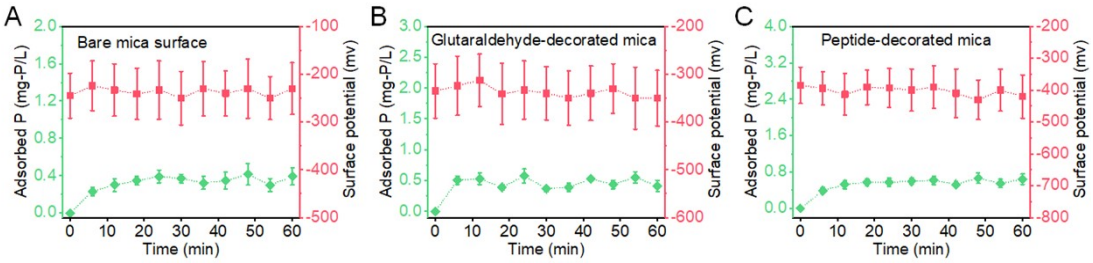

Figure S6. Quantification of adsorbed P and the corresponding Kelvin potential on (A) bare mica surface, (B) glutaraldehyde-decorated mica surface and (C) peptide-decorated mica surface with time after exposure to a simple P solution (100 mg/L KH_2PO_4; pH 5; 10 mM KCl).

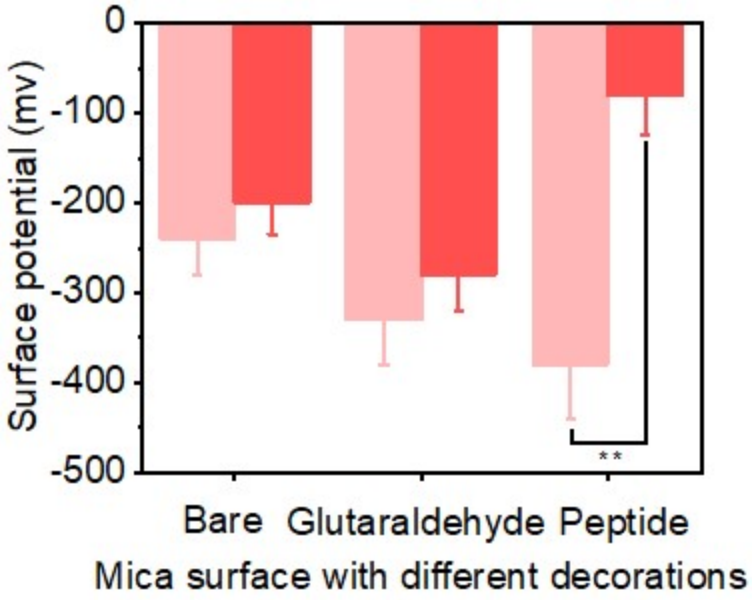

Figure S7. Quantification of the Kelvin potential on bare mica surface, glutaraldehyde-decorated mica surface and peptide-decorated mica surface before and after the introduction of 0.4 mM $CeCl_3$ (pH 5; 10 mM KCl).

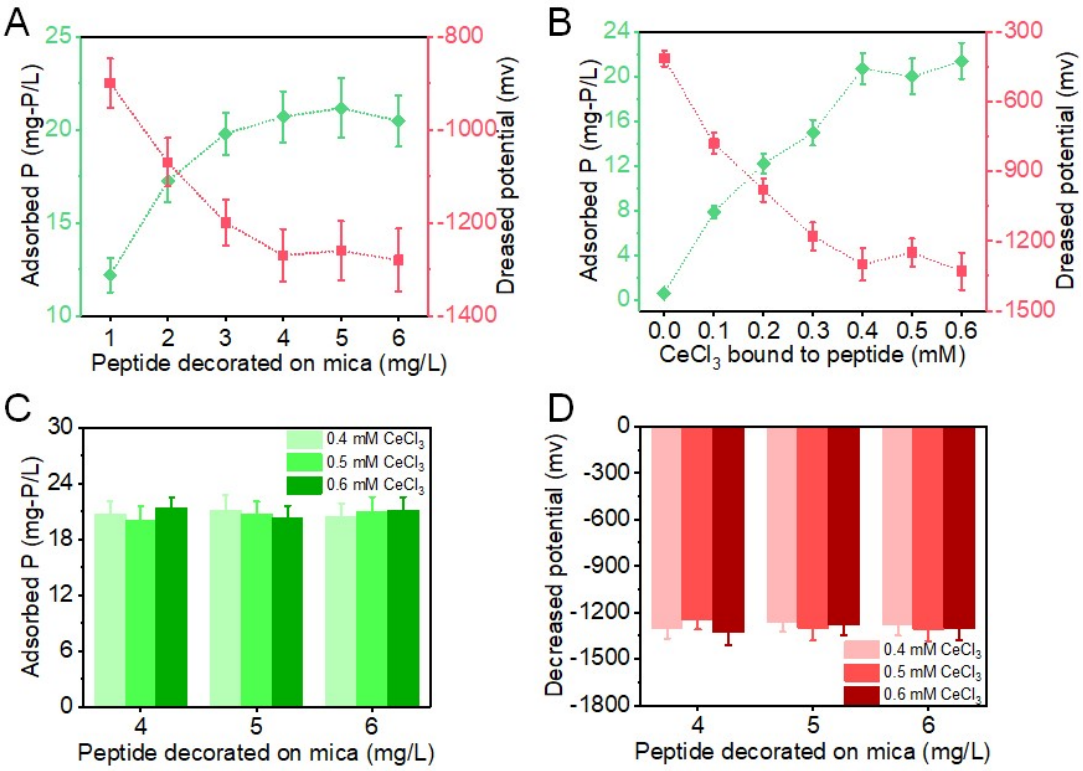

Figure S8. Quantification of adsorbed phosphate and decreased Kelvin potential on

mica surface with (A) decoration of different concentrations of peptide (1–6 mg/L) and binding of constant concentration of $CeCl_3$ (0.4 mM) and (B) decoration of constant concentration of peptide (4 mg/L); and binding of different concentrations of $CeCl_3$ (0.0–0.6 mM); and (C-D) decoration of different concentrations of peptide (4–6 mg/L) and binding of different concentrations of $CeCl_3$ (0.4–0.6 mM).

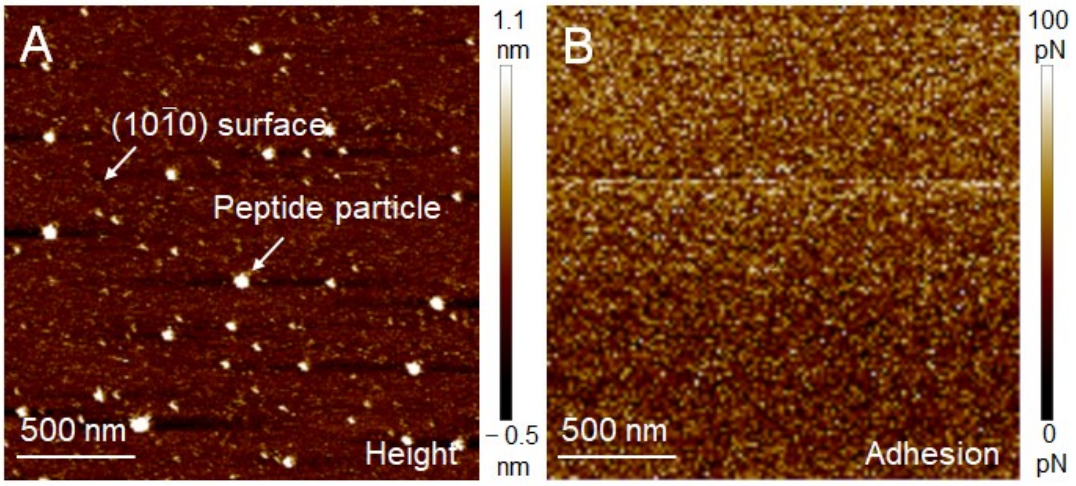

Figure S9. (A) AFM height imaging of peptide deposited on the (10$\bar{1}$0) surface of hematite, and (B) the corresponding adhesion mapping between phosphate group and (10$\bar{1}$0)/peptide, indicating there is no significance difference in adhesion force for phosphate group-peptide without Ce^{3+} binding compared to phosphate group-(10$\bar{1}$0).

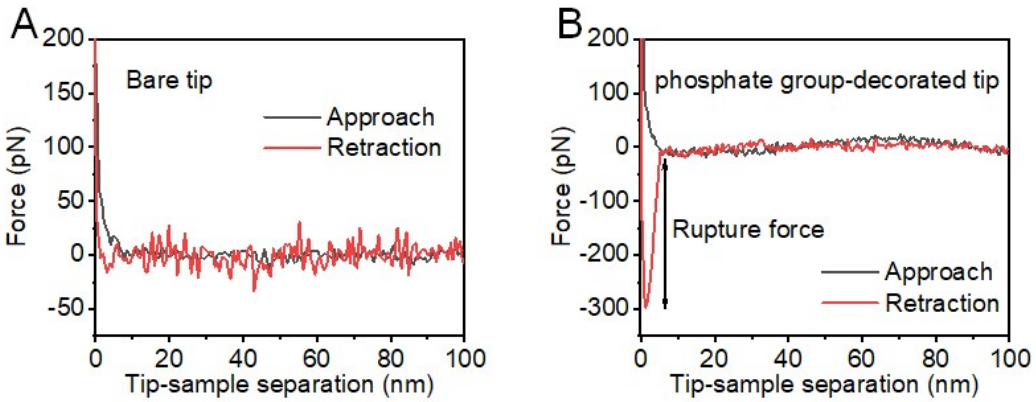

Figure S10. Representative force distance curves between (A) bare tip or (B) phosphate

group-decorated tip and the $(10\bar{1}0)$ surface of hematite.

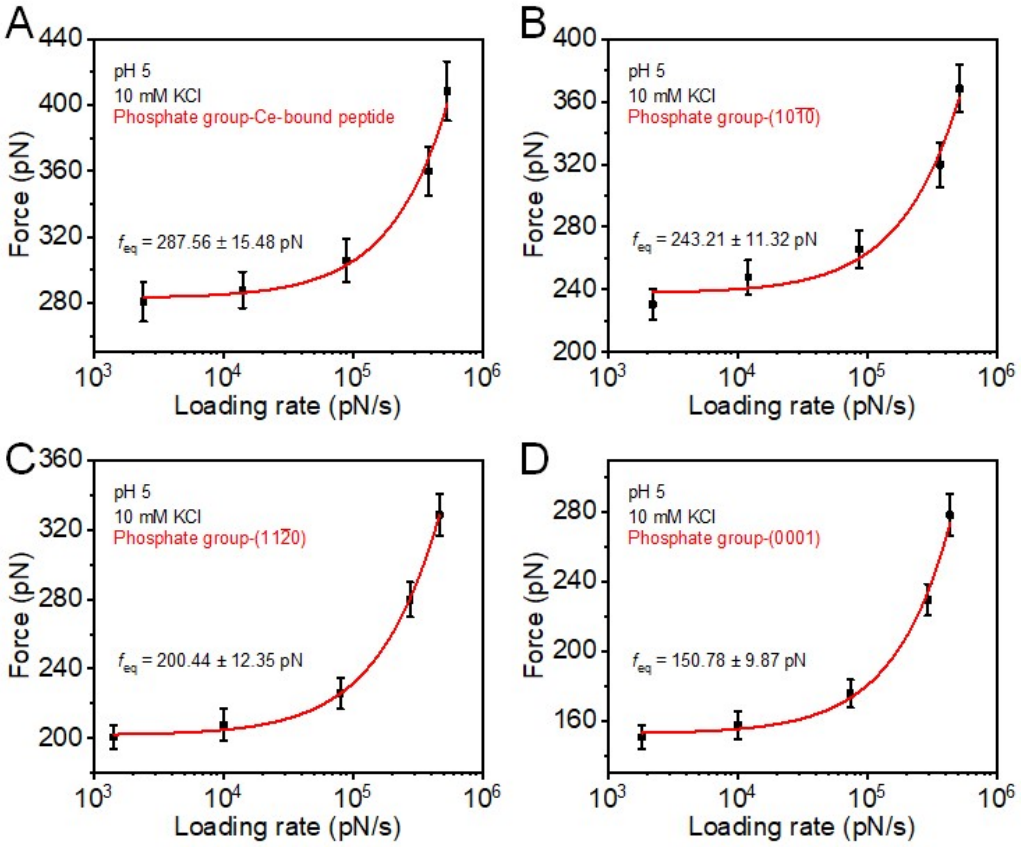

Figure S11. DFS of phosphate group binding to surfaces of (A) Ce-bound peptide decorated on mica, (B) $(10\bar{1}0)$, (C) $(11\bar{2}0)$ and (D) (0001) in a pH 5, 10 mM KCl solution.

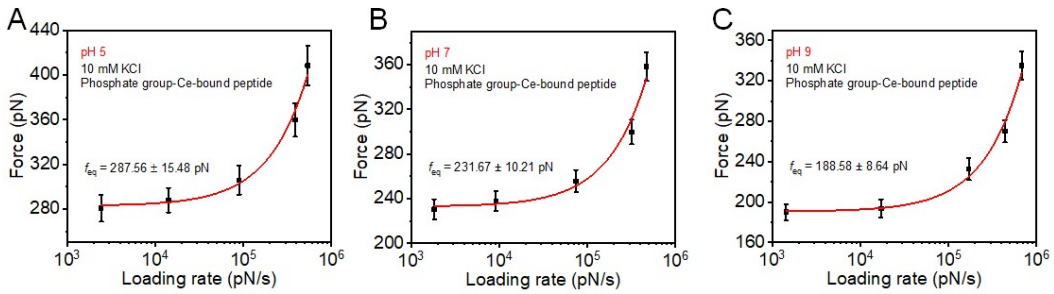

Figure S12. DFS of phosphate group binding to surface of Ce-bound peptide decorated on mica in a 10 mM KCl solution with different pH values of (A) 5 (B) 7 and (C) 9.

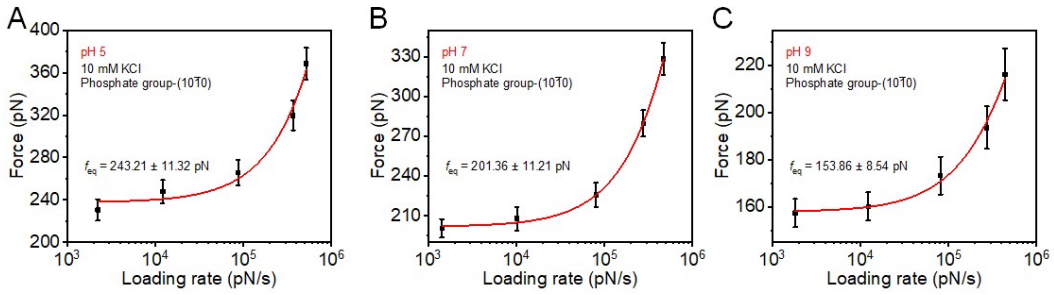

Figure S13. DFS of phosphate group binding to (10$\bar{1}$0) surface of hematite in a 10 mM KCl solution with different pH values of (A) 5 (B) 7 and (C) 9.

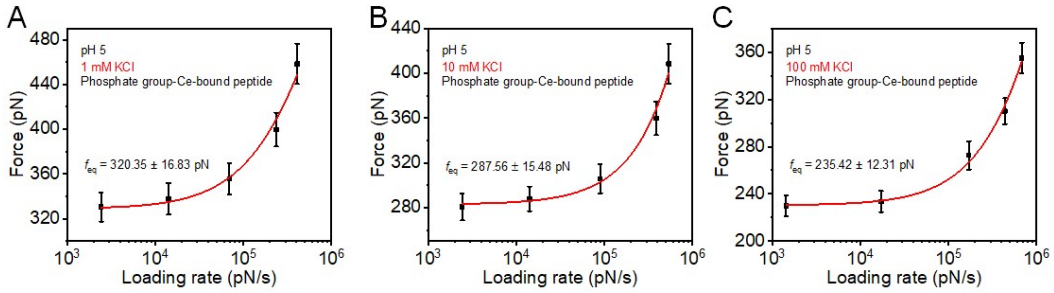

Figure S14. DFS of phosphate group binding to surface of Ce-bound peptide decorated on mica in a pH 5 solution with different KCl concentrations of (A) 1 mM (B) 10 mM and (C) 100 mM.

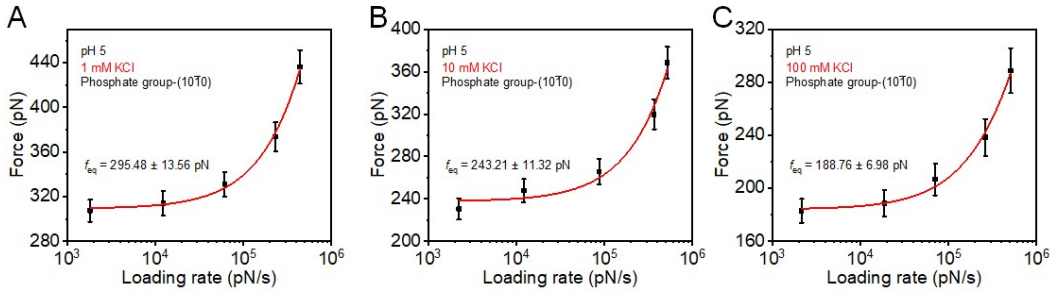

Figure S15. DFS of phosphate group binding to (10$\bar{1}$0) surface of hematite in a pH 5 solution with different KCl concentrations of (A) 1 mM (B) 10 mM and (C) 100 mM.

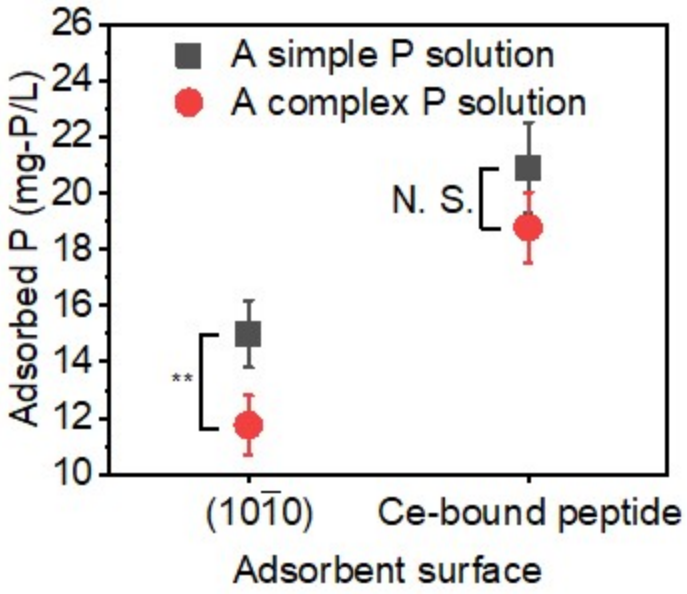

Figure S16. Significance analyses of adsorbed P on different adsorbent surfaces including (10$\bar{1}$0) and Ce-bound peptide after exposure to the simple/complex P solution.